

# Biodegradable Nanofibrous Polymeric Substrates for Generating Elastic and Flexible Electronics

Alireza Hassani Najafabadi, Ali Tamayol, Nasim Annabi, Manuel Ochoa, Pooria Mostafalu, Mohsen Akbari, Mehdi Nikkhah, Rahim Rahimi, Mehmet R. Dokmeci, Sameer Sonkusale, Babak Ziaie, and Ali Khademhosseini\*

The fabrication of electrical circuits on advanced elastomeric substrates has enabled the development of a new class of electronics with novel characteristics such as flexibility, biocompatibility, and degradability.<sup>[1]</sup> These characteristics have made these electronics suitable for an array of applications such as implantable devices,<sup>[2]</sup> smart wound dressings, sensors in food industry,<sup>[3]</sup> and epidermal sensors.<sup>[4]</sup> In the past few years, flexible electronics have been realized by patterning metals and organic conductors on the surface of thin films made from poly(dimethylsiloxane) (PDMS),<sup>[2,5]</sup> silk,<sup>[3,6]</sup> poly(imide),<sup>[7]</sup>

poly(4-vinylpyridine),<sup>[8]</sup> poly(styrene-block-butadiene-block-styrene),<sup>[9]</sup> and paper.<sup>[10]</sup> Other biodegradable polymers such as poly(lactic-co-glycolic) acid (PLGA)<sup>[11]</sup> have also been utilized for fabricating degradable electronics, which are known as physically transient electronics. In another example, natural compounds such as potato starch, gelatin, or caramelized glucose were used as the substrate for designing biodegradable organic field-effect transistors.<sup>[12]</sup>

Elastic electronics with capability of forming conformal contact to non-flat surfaces have been formed by patterning metallic microstrips on elastomers or degradable substrates.<sup>[4,13,14]</sup> This approach requires the utilization of an elastic and biodegradable substrate and a technique to maintain the contact between the conductive layer and the substrate without changing its physical properties. For example, in surface electromyography, where dermal sensors measure the electrical signals generated by skeletal muscles, the substrate should allow conformal contact to the skin while its mechanical characteristics should prevent interfering with the muscle induced motions.<sup>[15]</sup> The utilization of free standing microstrips also allows conformal contact between the metallic lines and the targeted surface.<sup>[14]</sup> However, the lack of a substrate limits their application to electrodes and sensors and prevents their utilization in advanced drug delivery systems or as smart wound dressings.

The suturability of polymer-based electronics is another important factor, which can affect their exploitation as implantable devices during surgeries to monitor the healing process of tissues or possible infections in the injury sites. In spite of the recent advances in the field of polymer-based electronics, there is a need for developing a substrate that meets all the aforementioned criteria while compatible with cost effective fabrication techniques.

A substrate that has attracted significant attention for fabricating cost-effective lab-on-a-chip devices as well as flexible electronics is paper.<sup>[16]</sup> Paper offers interesting physical properties including light weight and flexibility. It is also porous and permeable to air and liquids, which makes it an ideal substrate for rapid diagnostic tools. Various low-cost rapid fabrication strategies such as inkjet printing, screen printing, and contact printing have been devised for patterning conductive materials on paper-based substrates. However, paper-based devices are not elastic, losing their properties in aqueous environments, which makes them unsuitable as flexible devices for applications where substrate elasticity plays an important biomechanical role. Therefore, an elastic, flexible, and biocompatible polymeric substrate with a fibrous microstructure can replace paper for the applications that require biocompatibility, controlled biodegradability, and elasticity.

Dr. A. H. Najafabadi,<sup>[+]</sup> Dr. A. Tamayol,<sup>[+]</sup> Dr. N. Annabi,  
Dr. M. Akbari, Dr. M. Nikkhah,<sup>[++]</sup> Dr. M. R. Dokmeci,  
Prof. A. Khademhosseini  
Biomaterials Innovation Research Center  
Division of Biomedical Engineering  
Department of Medicine  
Brigham and Women's Hospital  
Harvard Medical School  
Cambridge, MA 02139, USA  
E-mail: alik@rics.bwh.harvard.edu



Dr. A. H. Najafabadi, Dr. A. Tamayol, Dr. N. Annabi,  
Dr. M. Akbari, Dr. M. Nikkhah, Dr. M. R. Dokmeci,  
Prof. A. Khademhosseini  
Harvard-MIT Division of Health Sciences and Technology  
Massachusetts Institute of Technology  
Cambridge, MA 02139, USA

Dr. A. H. Najafabadi  
Department of Chemistry  
Amirkabir University of Technology  
Tehran P.O. Box 1587-4413, Iran

Dr. N. Annabi, Dr. M. Akbari, Prof. A. Khademhosseini  
Wyss Institute for Biologically Inspired Engineering  
Harvard University  
Boston, MA 02115, USA

Prof. A. Khademhosseini  
Department of Physics  
King Abdulaziz University  
Jeddah, Saudi Arabia

M. Ochoa, R. Rahimi, Prof. B. Ziaie  
School of Electrical and Computer Engineering  
Birck Nanotechnology Center  
Purdue University  
West Lafayette, IN 47907, USA

P. Mostafalu, Prof. S. Sonkusale  
Department of Electrical and Computer Engineering  
Tufts University  
Medford, MA 02155, USA

<sup>[+]</sup>A. Hassani Najafabadi and A. Tamayol contributed equally to this work.

<sup>[++]</sup>Present address: School of Biological and Health Systems Engineering, Arizona State University, Tempe, AZ 85287, USA

DOI: 10.1002/adma.201401537

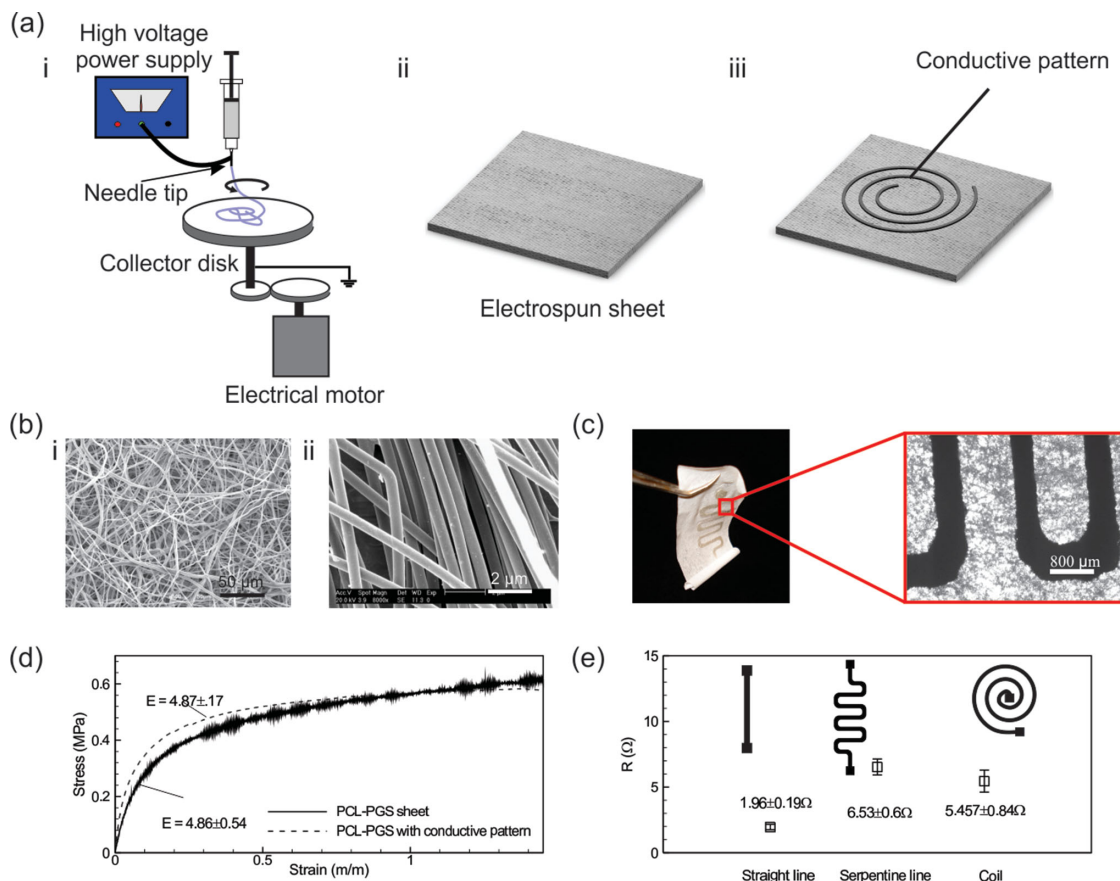


**Figure 1.** Fabrication and characterizations of PGS-PCL substrate-based electronics. (a) Schematic of the electrospinning setup used for fabricating sheets with uniform thickness (i,ii) and fabricating a conductive pattern by screen printing of silver ink on a substrate using a shadow mask (iii). (b) Representative SEM images of typical PGS-PCL electrospun sheets (with the ratio of 1:1), low magnification (i) and high magnification (ii). (c) A representative image of patterned electrospun sheet with a zoomed in micrograph showing the preservation of the PGS-PCL microstructure after the patterning process. (d) Representative strain-stress curves for a typical PGS-PCL electrospun sheet and a sheet containing a conductive pattern. (e) Electrical resistance of different patterns that indicates repeatability of the pattern formation on the surface of electrospun sheet (at least  $n = 6$  independent measurements).

Electrospinning is an approach that allows the fabrication of fibrous structures from various polymers (Figure 1(a)).<sup>[17]</sup> In electrospinning, a high electrical field is applied to a stream of prepolymer that breaks it into micro- and nano-sized filaments which are deposited on a collector to form a fibrous construct.<sup>[18]</sup> The physical properties of the fabricated structures (e.g., mechanical properties and microstructures) depend on the characteristics of the employed polymer as well as the fabrication parameters such as applied electrical field, solution viscosity, and the injection flow rate.<sup>[19]</sup> Electrospun sheets have been used for different applications including tissue engineering and drug delivery as various drugs can be loaded into the prepolymer before the electrospinning process to have a controlled release.<sup>[20]</sup> Here, we utilized electrospun elastic sheets of poly(caprolactone)-poly(glycerol sebacate) (PGS-PCL) substrates for engineering stretchable and biodegradable electronics (Figure 1b). We then created different conductive patterns using silver ink on the surfaces of the fabricated PGS-PCL sheets to engineer highly flexible and elastic electronics. These patterned substrates were used in various applications such as elastic and biocompatible heaters, temperature sensors,

and strain gauges as a proof-of-principle to demonstrate their practicality. The fabricated polymeric electrospun sheets hold great promise for engineering biodegradable elastic electronics if combined with biodegradable metals such as Mg.<sup>[6]</sup>

PGS is an elastomer that has been utilized as an elastic biodegradable material in cardiac tissue engineering.<sup>[21]</sup> The mechanical properties (elastic modulus, extensibility, and ultimate strength) of PGS can be tuned by blending it with PCL, which is a mechanically strong synthetic polymer.<sup>[22]</sup> Moreover, our group has recently shown that PGS-PCL mixtures with different compositions can be electrospun to form fibrous scaffolds for tissue engineering applications.<sup>[23,24]</sup> The degradation rate of the PGS-PCL substrate is a function of the ratio of the two polymers in the mixtures.<sup>[23]</sup> Here, we utilized a composition of 1:1 PGS-PCL for fabricating polymeric sheets. We used a custom-made drum with a rotational speed of approximately 1000 rpm to form electrospun sheets with a homogenous distribution of fibers. SEM images of a typical electrospun sheet demonstrated the random distribution of filaments as well as the homogeneity of the sheet (Figure 1b). The PGS-PCL electrospun sheets had similar morphology and physical

characteristics to conventional paper substrates. Thus, various techniques which have been developed for the fabrication of paper-based electronics can be implemented for patterning PGS-PCL sheets. We created conductive patterns on the surface of electrospun sheets by screen printing of silver ink through a shadow mask (stencil) (see the Experimental Section for details), which eliminated the need of using sophisticated equipment and facilities. The process of fabricating conductive patterns and microscopy images of typical patterns by screen printing using shadow mask is shown in Figure S1.

Silver ink is easy-to-implement and possesses antibacterial properties, which make it ideal for application in smart wound dressings and dermal patches. In general, the screen printing of silver ink on the PGS-PCL substrates did not affect their microstructure (Figure 1c). Conventional tensile tests performed on the fabricated electrospun substrates with and without the five pattern shows that patterning has an insignificant effect on the mechanical properties of the device (Figure 1d). The elastic moduli of the substrate and the patterned PGS-PCL sheets were  $4.86 \pm 0.54$  MPa and  $4.87 \pm 0.17$  MPa, respectively. These values are comparable to the elastic modulus of some native tissues such as skin dermis.<sup>[25]</sup> Also, all the samples behaved linearly with no plastic deformation within the first 10% strain range (Figure 1d).

We also investigated the repeatability of the fabrication process by measuring the electrical resistance of three patterns including a straight line (25 mm long and 1 mm wide), a serpentine pattern, and a spiral coil (Figure 1e). With the exception of the spiral coil, the variations in the electrical resistance of the rest of the fabricated designs were less than 10%.

An important advantage of PGS-PCL electrospun sheets is their suturability. We sutured two pieces of PGS-PCL sheets (15 mm  $\times$  15 mm each) and stretched the samples using a mechanical tester at the rate of 1 mm/min (Figure S2). No significant difference was observed in the stress-strain curves of the sutured samples compared to unsutured ones; the elastic modulus for sutured PGS-PCL samples was  $4.25 \pm 0.45$  MPa, which was comparable to the value obtained for the unsutured samples ( $4.86 \pm 0.54$  MPa).

To further characterize the physical properties (i.e., elasticity and flexibility) of the developed patterns, we fabricated serpentine silver lines on the surface of PGS-PCL sheets and measured their electrical conductivity upon stretching (details are provided in the Experimental Section). Our results indicated a variation of less than 10% in the electrical conductivity within a 6% strain (Figure 2a), which is comparable to the strain range tolerated by skin.<sup>[15]</sup> The variation in the electrical resistance is comparable with the results presented for composites of elastomeric electrospun fibers and silver nanoparticles.<sup>[9]</sup> The variation in electrical resistance was magnified beyond 6% strain, which was due to reduction of the number of nanoparticles in direct contact as the pattern was stretched. This observation is in-line with other studies that utilized composites of elastomers doped with conductive nanoparticles.<sup>[26]</sup> The dependence of electrical conductivity on tensile stress stems from the fact that the deformation of the substrate separates the conductive silver particles and creates cracks in the pattern. It is anticipated that such variations can be significantly reduced by fabricating metallic patterns through sputtering or vapor deposition. We also measured the stress-strain curves and the electrical conductivity of

the patterned samples that were exposed to a cyclic stretch (4% strain) after each cycle (for details please refer to the Experimental Section). Our results indicated that the electrical resistance did not change within the first few cycles and the variations became more pronounced after 20 cycles (Figure 2b). However, the stress-strain curves showed slight variation after the third cycle. This observation confirms the elasticity of the PGS-PCL platform and suggests that by utilization of a ductile electrically conductive material the electrospun sheets can be used in designing dermal sensors and wound dressings which undergo cyclic loading during their operation.<sup>[15]</sup> PGS-PCL substrate offers combined biodegradability, elasticity, and flexibility, which distinguishes it from other counterparts used in the literature.

Although the main goal of the present study is the introduction of the polymeric substrate, we demonstrated the flexibility of the fabricated patterns by wrapping PGS-PCL sheets patterned with a straight silver line around Teflon cylinders that were 1, 5, 12.5, and 15 mm in diameter while measuring their electrical resistance. Depending on the position of the silver patterns with respect to the Teflon cylinders, the silver line can experience compression or tension. In Figure 2c, the radius of curvatures for cases in which the conductive pattern is compressed, is shown by a negative sign. It can be seen that the structure remained conductive over the entire range of curvature radii. Since the substrate is elastic and flexible on its own, by adaptation of other fabrication techniques such as soft lithography<sup>[8]</sup> or growing conductive nanoparticles on the substrate,<sup>[9]</sup> the flexibility and elasticity of the conductive patterns can be enhanced.

We first tested the stability of the employed silver ink in phosphate buffered saline (PBS). We patterned silver ink on the surface of a glass slide and let the pattern to dry for 24 h. The samples were then placed in PBS and the electrical conductivity was measured over 10 h (Figure S3). The results suggest that the electrical conductivity of the silver ink did not change over 10 h. We then tested the electrical performance of electrospun nanofibrous sheets with a serpentine silver line in different environments including air at room temperature, NaOH (0.01 M), a basic solution to increase degradation rate of PGS-PCL, PBS conventionally used in biological experiments, and cell culture medium (Figure 3a). We also measured the electrical resistance of a conductive pattern in cell culture medium over 14 days. It was demonstrated that the electrical resistance of these patterns only changed by approximately 15% (Figure 3b), which may be due to the physical stability of the PGS-PCL substrates in these conditions.

To investigate the effect of the PGS-PCL degradation on the electrical properties of the conductive pattern, we placed nanofibrous substrates with a serpentine silver pattern in NaOH (0.01M) and PBS solutions at 37 °C and measured their electrical resistance and their mass weight over 14 days. Figure 3c shows images of the micropatterned sheets before and after the complete degradation of the substrate after 30 days. The variation in the electrical resistance of the patterns during the first 10 days of experiment was less than 10% (Figure 3d, f). Furthermore, we noticed a more gradual degradation of the fabricated conductive pattern in PBS (1X) over 14 days. We observed a 20% and 15% mass loss in the fabricated patterns incubated in PBS and NaOH (0.01M) solution, respectively (Figure 3e,g).

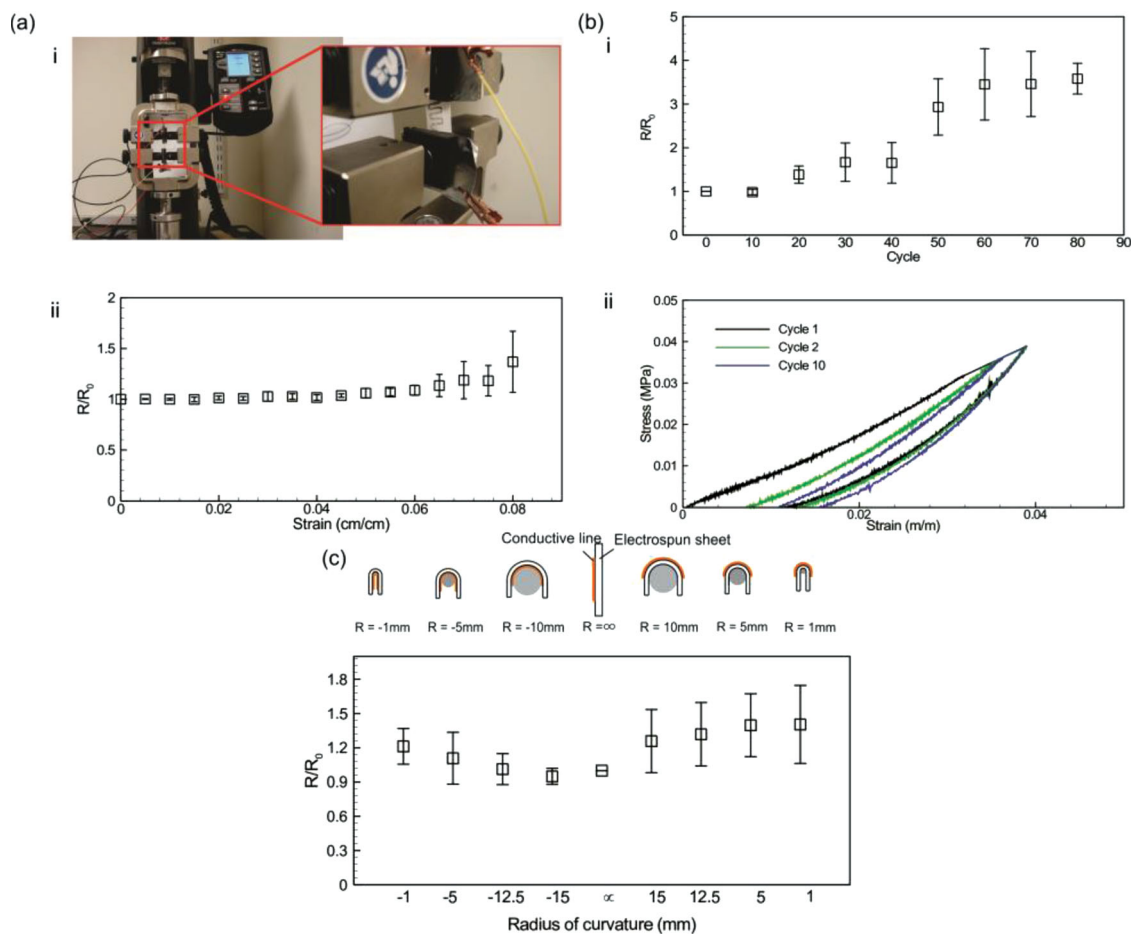


**Figure 2.** Elasticity and flexibility of the fiber-based electronic circuits. (a) Variation of the electrical resistance of the serpentine line as a function of mechanical strain. (i) Images show the setup used for stretching the sample and measuring its tensile mechanical properties while monitoring its electrical resistance. (ii) The values of electrical resistance of the stretched patterns ( $R$ ) non-dimensionalized with the values in the unstretched condition ( $R_0$ ); the presented results are the average of (at least  $n = 6$ ) independent measurement. (b) Effect of cyclic load on the electrical resistance (i) and stress-strain curve (ii) of the fabricated pattern; the device was stretched by 4% of its original length and then released to its original length with a rate of 1 cycle/minute. (c) Schematic diagram of patterned silver on sheet wrapped around curved surfaces with different curvature radii (top) and the ratio of the measured electrical resistance after cyclic load ( $R$ ) to the initial electrical resistance ( $R_0$ ) of patterned silver on electrospun sheet versus the curve diameter to which the sheet is turned (bottom).

Even when the PGS-PCL platform was completely degraded under aggressive conditions using 0.5M NaOH, the architecture and electrical functionality of the fabricated systems were preserved. These results confirmed that PGS-PCL electrospun sheets could be utilized for designing degradable electronics while the overall electronic performance can be maintained during the degradation process.

Another application of our fabricated PGS-PCL platform is as smart dermal patches and wound dressings capable of sensing, releasing drugs, and maintaining the surface temperature. To confirm the biocompatibility of this platform, we seeded silver patterned samples with NIH 3T3 fibroblasts and incubated them in cell culture medium at 37 °C for 3 days. Cell viability was assessed by performing a live/dead assay. As shown in Figure S4a, more than 95% of the cells remained viable after 3 days of culture. This observation confirmed that the PGS-PCL platform and the patterned silver ink did not induce cellular cytotoxicity. In addition, we investigated the cellular morphology through staining against F-actin after 3 days

of culture (Figure S4b). Our staining showed that cells spread over the entire surface of the PGS-PCL platform with the exception of the area covered by the electrodes, which can prevent cell growth from interfering with the electrical characteristics of the conductive pattern.

Monitoring the tissue temperature can provide information about potential local inflammations or infections. To demonstrate the utility of this platform as a temperature sensor, we patterned silver ink in a spiral pattern on the surface of PGS-PCL sheets and correlated the changes in the surrounding temperature with electrical resistance. The patterned sheets were placed on the surface of a heater and the measured electrical resistance was calibrated with the surface temperature (Figure 4a,i,ii). Our results indicated a linear relationship between the electrical resistance and temperature in the range of 27 °C to 40 °C, which is of relevance for biological samples.

Wound patches equipped with a heating system can elevate the skin temperature locally or can be combined with temperature sensitive polymers to activate the drug release. We used a

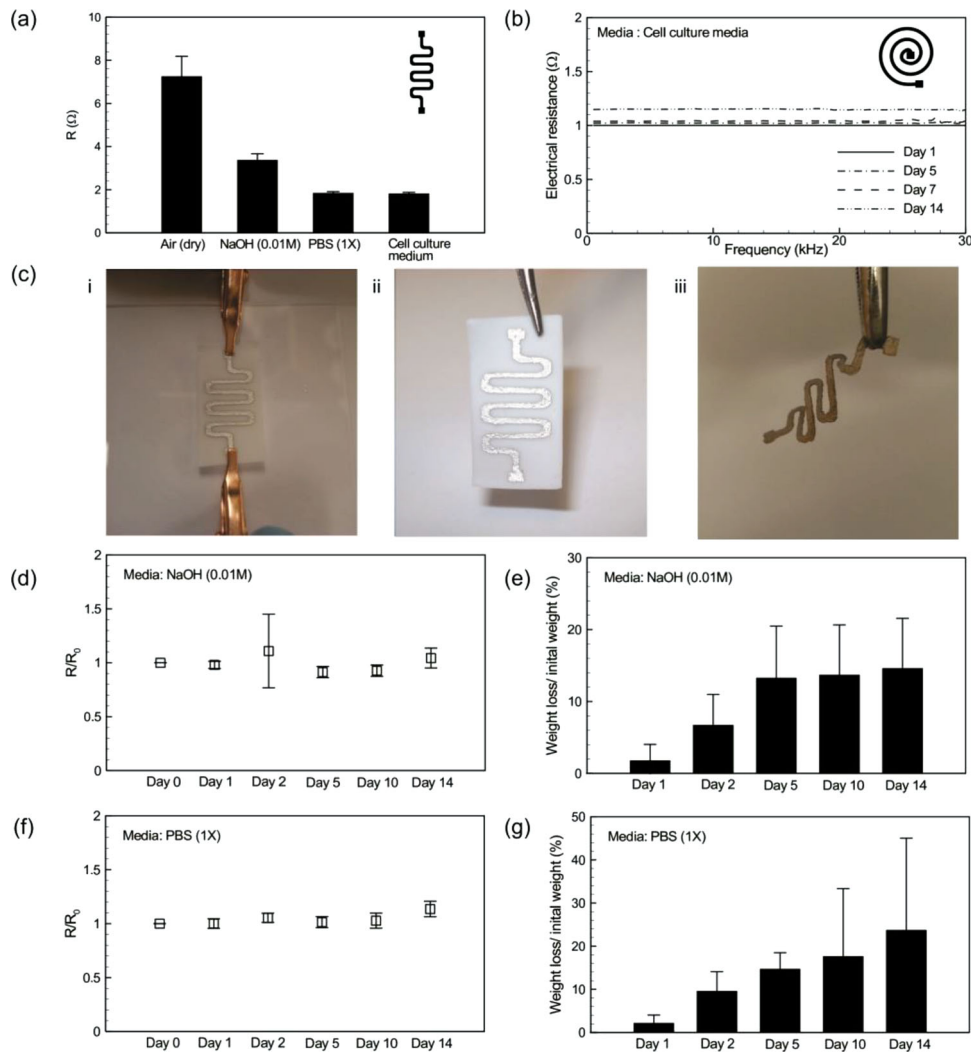


**Figure 3.** Electrical resistance of the fabricated devices in various environmental conditions. (a) The effect of media on the measured electrical resistance of serpentine lines patterned on the surface of PGS-PCL sheets; air represents the dry condition. (b) The electrical resistance of a coil patterned on the surface of an electrospun sheet inside cell media and incubator at 37 °C coil seeded with 3T3 cells over 14 days. (c) Images showing the degradation of the device inside a solution of 0.5 M NaOH. (i) a typical device connected to grips for measuring its electrical resistance; (ii) image of a typical conductive pattern on the surface of an electrospun sheet before degradation. (iii) the image of the same structure after complete degradation of the polymeric substrate which left behind the conductive pattern. (d,f) Electrical resistance ( $R$ ) of the patterned electrodes over 14 days in 0.5 mM NaOH and PBS non-dimensionalized with respect to their original resistance after fabrication ( $R_0$ ); the results are the average of  $n = 6$  independent measurements. (e,g) Mass loss of the device over 14 days in 0.01 mM NaOH and PBS; the results are the average of  $n = 6$  independent measurements.

similar design as a heater and placed a film thermometer on its surface. We applied a constant voltage using a power supply until the surface temperature reached 37 °C and an “N” sign appeared on the thermometer (Figure 4a<sub>iii</sub>). We used an in house micro-controller and controlled the generated heat by monitoring the surface temperature of the heater over 30 minutes (Figure S5).

A potential application of the designed PGS-PCL substrate is in surface myography in which the contraction of skeletal muscles can be assessed. Another potential application that requires measuring strain rate is the smart wound dressings for treating chronic wounds, where the rate and quality of healing can be improved by applied mechanical forces.<sup>[27]</sup>

To demonstrate the utility of our engineered system for this application, we also designed a wireless strain sensor in which  $\text{Fe}_3\text{O}_4$  was screen-printed onto the PGS-PCL substrate

(Figure 4b). When the patterned substrate was placed over a polyimide-insulated copper coil, the  $\text{Fe}_3\text{O}_4$  behaved as the core of the inductor coil and generated a high magnetic permeability near the coil, thus raising its inductance value. Upon stretching the substrate, the  $\text{Fe}_3\text{O}_4$  spots expanded away from each other. This reduction in the density of  $\text{Fe}_3\text{O}_4$  resulted in a decreased magnetic permeability, which on its own lowered the coil inductance. The changes of inductance in response to strain can be monitored wirelessly by measuring the resonant frequency.

The resonant frequency of the coil was monitored using a spectrum analyzer as the substrate was stretched using a micro-manipulator. The experimental results indicated a positive correlation between the applied strain and its inductance value. This trend was due to the decreasing of  $\text{Fe}_3\text{O}_4$  density during the stretching process, which in turn lowered the coil inductance

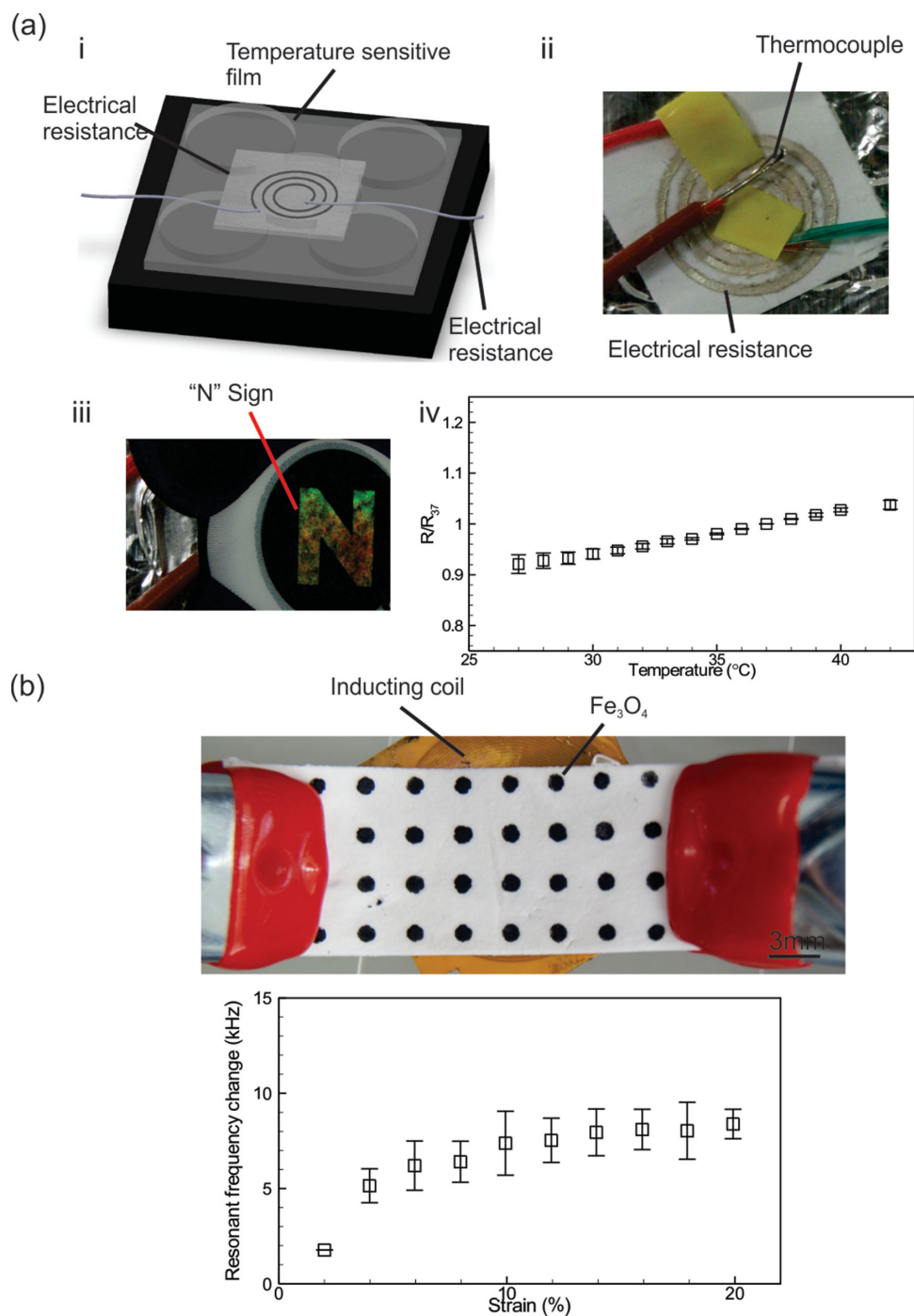


**Figure 4.** Application of the PGS-PCL platform in functionalized wound patches. (a) The use of the platform as a bioresorbable temperature sensor and heater (i, ii). As a heater the device was covered with a temperature sensitive film (thermometer strip) and electrical voltage was applied to the conductive pattern which was used as a resistor to generate heat. The schematic of the system is shown (i) along with an image of the temperature sensitive film indicating "N" sign associated with 37 °C (iii); in the case of temperature sensor, the device was mounted on the surface of a heater and the conductive pattern was connected to a multimeter to measure its electrical resistance while the surface temperature was simultaneously measured with a T-type thermocouple (iv). The resistance in different temperatures ( $R$ ) is non-dimensionalized with respect to the resistance at 37 °C ( $R_{37}$ ). (b)  $Fe_3O_4$  paste screen-printed onto PGS-PCL sheets to create circular patterns in ordered arrangements. The patterned substrate was clamped to a micro-manipulator and was placed on top of a polyimide-insulated copper coil connected to an impedance analyzer. The variation in the resonant frequency of the coil was measured and correlated to the substrate strain.

and created a higher resonant frequency. The fabricated sensor offered strain measurements with an average sensitivity of 0.7% kHz between 0–10% strain and 0.1% kHz between 10–20%

strain, which was comparable to other wireless antenna-based sensors.<sup>[28]</sup> The strain range is also comparable to other flexible strain sensors.<sup>[8]</sup> The working mechanism of the sensors

is based on strain-controlled modulation of the inductance of a coil, which depends on the magnetic permeability of its vicinity. Since this value is very similar for both, air and water, the sensors can be expected to function in a wet environment. Similar sensing schemes have previously been used successfully in wet environments, thus, it is expected that the present sensor will be functional in wet conditions, unlike antenna-based devices with sensitive fringe capacitance.<sup>[29]</sup> For future implementations, the sensor can be further improved by geometric customization and increasing the resolution of screen printed patterns.

In conclusion, we introduced polymeric nanofibrous sheets made from PGS-PCL as platforms for designing bioresorbable and elastic electronics. These substrates offer many interesting characteristics including elasticity, suturability, and gradual degradability. The PGS-PCL substrate, like paper, is a mesh of thin fibers with wicking properties that enables its compatibility with fabrication techniques commonly used in paper electronics. These include depositing electrically conductive traces by screen printing or inkjet printing of metallic inks, patterning, or machining using laser.<sup>[30]</sup> As an example, here we utilized shadow masks to create conductive patterns from silver ink and  $\text{Fe}_3\text{O}_4$  on the PGS-PCL substrate. We then demonstrated the flexibility and elasticity of the fabricated platform and conductive patterns and also tested the effect of environmental conditions on the degradation rate and electrical characteristics of engineered devices. It was observed that despite the gradual degradation of PGS-PCL substrate due to hydrolysis, the electrical performance was preserved.

In addition, the PGS-PCL sheets patterned with silver were compatible with cell culture, confirming the suitability of our engineered platform for biomedical applications. As a proof-of-principle demonstration, we fabricated temperature sensors, heaters, and strain sensors on PGS-PCL substrates. The electrical resistance had a linear relationship with temperature. Moreover, we noticed that the systems could sustainably generate heat and maintain their surface temperature over a period of time. Finally, we screen printed  $\text{Fe}_3\text{O}_4$  dots on PGS-PCL substrate to create a wireless strain sensor. The strain rate was determined through measuring the variation in the inductance of an insulated coil.

This study paves the way for merging the advancements in the areas of paper-based electronics and biodegradable devices. In addition, it opens new opportunities for fabricating biocompatible and elastic devices.

## Experimental Section

**Materials:** PCL (MW 70000–90000), anhydrous chloroform, and ethanol were purchased from Sigma-Aldrich (St. Louis, MO, USA). PGS (MW 12000) was synthesized following the procedure previously described.<sup>[23]</sup> Briefly, PGS was synthesized by polycondensation of glycerol and sebacic acid (Sigma-Aldrich, St. Louis, MO, USA) under nitrogen atmosphere at 120 °C for 24 h. The pressure was then reduced gradually from 1 Torr to 40 mTorr over 24 h. The synthesized PGS was used without any further purification. Fast drying silver paint was purchased from Ted Pella Inc, USA. Dulbecco's modified Eagle medium (DMEM), 0.05% trypsin-EDTA (1X), antibiotics (Penicillin/Streptomycin), and fetal bovine serum (FBS) were purchased from Invitrogen (Carlsbad, CA, USA). A final DMEM solution was prepared with 10% FBS and 1% antibiotics (penicillin/streptomycin). LIVE/DEAD Viability/Cytotoxicity Kit, for mammalian cells was purchased from

Invitrogen (Carlsbad, CA, USA). Other chemicals were purchased from Sigma Aldrich (St. Louis, MO, USA) unless mentioned otherwise.

**Electrospinning Process:** A conventional electrospinning set-up comprised of a syringe pump, high voltage supply, and a collector plate was utilized to fabricate PGS-PCL sheets. The tip of the syringe was connected to the positive electrode of the high voltage power supply and fibers were collected on a disk with the rotating speed of 1000 rpm to create a sheet with uniform fiber distribution. The disk was covered with an aluminum foil, which was grounded and coated with a layer of mineral oil to facilitate the detachment of the electrospun sheet.

PGS and PCL were dissolved at the ratio of 1:1 in anhydrous chloroform: ethanol (9:1) mixture (the total polymer concentration was kept constant at 20% w/v). An electrical field of 20 kV over a distance of 18 cm (the distance between the needle and the collector) was applied. The flow rate of the prepolymer was set to 2 mL/h and a 21 G needle was used during electrospinning process. The substrates were spun for 20 min to have a thickness of approximately 500  $\mu\text{m}$ . The substrates were then dried in a desiccator overnight to remove any remaining solvent prior to further use.

**Patterning of the Electrospun Sheets:** Electrically conductive patterns were fabricated from silver ink using a screen printing method. In this method, electrospun sheets were covered with a shadow mask, which was previously prepared by a laser cutter (Versalaser, VLS2.30, 10% power, 50% speed). Then, silver ink was added to one side of the mask and drawn using a PDMS substrate to cover the whole area of the shadow mask (similar to filling in painting, Figure S1). The PGS-PCL sheets patterned with silver ink was then placed in a desiccator for 1 h and allowed to completely cure at room temperature for 24 hr. Finally, the shadow masks were removed from the sheets leaving the patterned electrical circuit on the electrospun sheets. The coated sheets were placed in a desiccator for future measurements.

**Mechanical Testing:** The mechanical properties of prepared electrode with different methods and patterns were measured using an Instron 5542 mechanical tester (Norwood, MA, USA) with a 1kN load cell. Electrospun patterned sheets were dried for at least 24 h in a vacuum desiccator to ensure the complete removal of solvent and they were subsequently cut to rectangular shapes (10  $\times$  50 mm). Each Specimen was inserted into the grips with a 10 mm gauge length. During the uniaxial test, the initial strain rate was set as 2.5% of the original test regional length and the samples were stretched at a constant rate of 0.5 mm/min. The slope of the stress-strain curve in the linear region (0–5% strain) was determined as a measure of the Young's modulus. Values were reported as mean  $\pm$  standard deviation of the measurements for 5 samples.

Similarly, the mechanical properties of patterned structures were measured. In this case, patterns were created as described previously and the patterned structures were cut and placed in desiccators until the experiments. For cyclic tensile tests, a 10 N load cell was used and a linear velocity of 0.5 mm/min was applied. The maximum strain at each cycle was set to 5%. The experiments were conducted on 3 samples for maximum of 80 cycles. After each 10 cycles, the values of electrical conductivity were measured.

**Designing the Wireless Strain Sensor:** An aqueous paste of  $\text{Fe}_3\text{O}_4$  (obtained from Sigma Aldrich) was screen-printed onto the substrate using a laser-machined 100  $\mu\text{m}$ -thick PET film as a mask. The pattern on the mask comprised a rectangular array of 1 mm-diameter holes spaced 1.5 mm from each other defined with a laser engraver (Universal Laser Systems, Scottsdale, AZ). The iron oxide paste was allowed to dry at room temperature over night before testing. For testing, the patterned substrate was clamped to a micro-manipulator and suspended over a polyimide-insulated copper coil connected to an HP4294A impedance analyzer (Agilent Technologies, CA). The resonant frequency of the coil was monitored as the substrate strain was increased using the micro-manipulator.

**Degradation:** Patterned electrospun sheets were placed in a six-well plate with 5 mL of PBS with 0.01% (w/v) of NaOH (Sigma-Aldrich W1, USA). Samples were incubated in NaOH solution at 37 °C for 1, 2, 5, 10, and 14 days. After each time point, the NaOH solution was removed, without disturbing the undigested polymer. The remaining sheets were washed with PBS, and then the excess liquid was removed and samples

were weighted. The degradation rate was calculated as the ratio of the weight after digestion to the original weight of untreated sheets.

**Scanning Electron Microscopy (SEM):** The SEM images of metal electrodes and constructed electrodes were acquired using a FEI/Philips XL30 FEG ESEM (15 KV) to determine the structural features of the fabricated electrospun substrates. Lyophilized samples were mounted on aluminum stubs using conductive carbon paint, then gold coated prior to SEM analysis.

**Cell Culture:** NIH 3T3 fibroblast cells were purchased from American Type Culture Collection (ATCC) (Manassas, VA, USA). Cells were grown in 5% CO<sub>2</sub> and 37 °C supplemented with DMEM containing 10% fetal bovine serum (FBS) and 1% penicillin/streptomycin. Cells were passaged every 3 days, cell culture medium was changed every 3 days to maintain experimental consistency.

## Supporting Information

Supporting information is available from the Wiley Online Library or from the author.

## Acknowledgements

The authors declare no conflict of interests in this work. A.T., M.O., P.M., R.R., M.R.D., S.S., B.Z., and A.K. acknowledge funding from the National Science Foundation (EFRI-1240443), the office of Naval Research Young National Investigator Award, and the National Institutes of Health (HL092836, DE019024, EB012597, AR057837, DE021468, HL099073, EB008392). M. A. and A. T. acknowledge NSERC Postdoctoral fellowships. N.A. acknowledges the support from the National Health and Medical Research Council.

Note: The affiliations and the acknowledgements were updated on September 1, 2014, after initial online publication. Several other corrections were also made to the manuscript, including in the caption to Figure 2a to reflect resistance; in the caption to Figure 3e,g, where the concentration was updated to 0.01 mM; and in the Materials section of the Experimental Section, where the reference number was corrected.

Received: April 4, 2014

Revised: May 26, 2014

Published online: July 19, 2014

- [1] M. Muskovich, C. J. Bettinger, *Adv. Healthcare Mater.* **2012**, *1*, 248.
- [2] D.-H. Kim, S. Wang, H. Keum, R. Ghaffari, Y.-S. Kim, H. Tao, B. Panilaitis, M. Li, Z. Kang, F. Omenetto, Y. Huang, J. A. Rogers, *Small* **2012**, *8*, 3263.
- [3] H. Tao, M. A. Brenckle, M. Yang, J. Zhang, M. Liu, S. M. Siebert, R. D. Averitt, M. S. Mannoor, M. C. McAlpine, J. A. Rogers, *Adv. Mater.* **2012**, *24*, 1067.
- [4] D.-H. Kim, N. Lu, R. Ma, Y.-S. Kim, R.-H. Kim, S. Wang, J. Wu, S. M. Won, H. Tao, A. Islam, K. J. Yu, T.-i. Kim, R. Chowdhury, M. Ying, L. Xu, M. Li, H.-J. Chung, H. Keum, M. McCormick, P. Liu, Y.-W. Zhang, F. G. Omenetto, Y. Huang, T. Coleman, J. A. Rogers, *Science* **2011**, *333*, 838.
- [5] J.-H. Lee, K. Y. Lee, M. K. Gupta, T. Y. Kim, D.-Y. Lee, J. Oh, C. Ryu, W. J. Yoo, C.-Y. Kang, S.-J. Yoon, J.-B. Yoo, S.-W. Kim, *Adv. Mater.* **2013**.
- [6] S.-W. Hwang, H. Tao, D.-H. Kim, H. Cheng, J.-K. Song, E. Rill, M. A. Brenckle, B. Panilaitis, S. M. Won, Y.-S. Kim, Y. M. Song, K. J. Yu, A. Ameen, R. Li, Y. Su, M. Yang, D. L. Kaplan, M. R. Zakin, M. J. Slepian, Y. Huang, F. G. Omenetto, J. A. Rogers, *Science* **2012**, *337*, 1640.
- [7] a) T. Sekitani, U. Zschieschang, H. Klauk, T. Someya, *Nat. Mater.* **2010**, *9*, 1015; b) Y. Zhang, S. Wang, X. Li, J. A. Fan, S. Xu, Y. M. Song, K.-J. Choi, W.-H. Yeo, Woosik Lee, S. N. Nazaar, B. Lu, L. Yin, K.-C. Hwang, J. A. Rogers, Y. Huang, *Adv. Funct. Mater.* **2013**, *24*, 2028.
- [8] M. Park, J. Im, J. Park, U. Jeong, *ACS Appl. Mater. Interfaces* **2013**, *5*, 8766.
- [9] M. Park, J. Im, M. Shin, Y. Min, J. Park, H. Cho, S. Park, M.-B. Shim, S. Jeon, D.-Y. Chung, J. Bae, J. Park, U. Jeong, K. Kim, *Nat. Nanotechnol.* **2012**, *7*, 803.
- [10] a) H. Tao, L. R. Chieffo, M. A. Brenckle, S. M. Siebert, M. Liu, A. C. Strikwerda, K. Fan, D. L. Kaplan, X. Zhang, R. D. Averitt, *Adv. Mater.* **2011**, *23*, 3197; b) W. J. Hyun, O. O. Park, B. D. Chin, *Adv. Mater.* **2013**, *25*, 4729.
- [11] C. J. Bettinger, Z. Bao, *Adv. Mater.* **2010**, *22*, 651.
- [12] M. Irimia-Vladu, P. A. Troshin, M. Reisinger, L. Shmygleva, Y. Kanbur, G. Schwabegger, M. Bodea, R. Schwödiauer, A. Mumyatov, J. W. Fergus, V. F. Razumov, H. Sitter, N. S. Sariciftci, S. Bauer, *Adv. Funct. Mater.* **2010**, *20*, 4069.
- [13] K. Fujimoto, G. Bonmassar, A. J. Golby, *Plos ONE* **2012**, *7*, e41187.
- [14] D.-H. Kim, J. Viventi, J. J. Amsden, J. Xiao, L. Vigeland, Y.-S. Kim, J. A. Blanco, B. Panilaitis, E. S. Frechette, D. Contreras, D. L. Kaplan, F. G. Omenetto, Y. Huang, K.-C. Hwang, M. R. Zakin, B. Litt, J. A. Rogers, *Nat. Mater.* **2010**, *9*, 511.
- [15] J.-W. Jeong, W.-H. Yeo, A. Akhtar, J. J. S. Norton, Y.-J. Kwack, S. Li, S.-Y. Jung, Y. Su, W. Lee, J. Xia, H. Cheng, Y. Huang, W.-S. Choi, T. Bretl, J. A. Rogers, *Adv. Mater.* **2013**, *25*, 6839.
- [16] a) A. C. Siegel, S. T. Phillips, M. D. Dickey, N. Lu, Z. Suo, G. M. Whitesides, *Adv. Funct. Mater.* **2010**, *20*, 28; b) J. L. Delaney, C. F. Hogan, J. Tian, W. Shen, *Anal. Chem.* **2011**, *83*, 1300; c) P. Mostafalu, S. Sonkusale, *Biosens. Bioelectron.* **2014**, *54*, 292; d) P. Mostafalu, S. Sonkusale, "Paper-based super-capacitor using micro and nanoparticle deposition for paper-based diagnostics", presented at *Sensors 2013 IEEE*, 3–6 Nov. 2013, **2013**.
- [17] A. Tamayol, M. Akbari, N. Annabi, A. Paul, A. Khademhosseini, D. Juncker, *Biotechnol. Adv.* **2013**, *31*, 669.
- [18] N. Annabi, A. Tamayol, J. A. Uquillas, M. Akbari, L. E. Bertassoni, C. Cha, G. Camci-Unal, M. R. Dokmeci, N. A. Peppas, A. Khademhosseini, *Adv. Mater.* **2014**, *26*, 85.
- [19] A. Greiner, J. H. Wendorff, *Angew. Chem. Int. Ed.* **2007**, *46*, 5670.
- [20] a) E.-R. Kenawy, G. L. Bowlin, K. Mansfield, J. Layman, D. G. Simpson, E. H. Sanders, G. E. Wnek, *J. Controlled Release* **2002**, *81*, 57; b) A. Y. A. Kaassis, N. Young, N. Sano, H. A. Merchant, D.-G. Yu, N. P. Chatterton, G. R. Williams, *J. Mater. Chem. B* **2014**, *2*, 1400.
- [21] a) D. Motlagh, J. Yang, K. Y. Lui, A. R. Webb, G. A. Ameer, *Biomaterials* **2006**, *27*, 4315; b) M. Kharaziha, M. Nikkhal, S.-R. Shin, N. Annabi, N. Masoumi, A. K. Gaharwar, G. Camci-Unal, A. Khademhosseini, *Biomaterials* **2013**, *34*, 6355.
- [22] S. Salehi, T. Bahners, J. S. Gutmann, S. L. Gao, E. Mader, T. A. Fuchsluger, *RSC Adv.* **2014**, *4*, 16951.
- [23] a) S. Sant, C. M. Hwang, S.-H. Lee, A. Khademhosseini, *J. Tissue Eng. Regen. Med.* **2011**, *5*, 283; b) S. Sant, D. Iyer, A. Gaharwar, A. Patel, A. Khademhosseini, *Acta Biomater.* **2012**, *9*, 5963.
- [24] N. Masoumi, B. L. Larson, N. Annabi, M. Kharaziha, B. Zamanian, K. S. Shaperro, A. T. Cubberley, G. Camci-Unal, K. B. Manning, J. E. Mayer, A. Khademhosseini, *Adv. Healthc. Mater.* **2014**, n/a.
- [25] J. L. Gennisson, T. Baldewick, M. Tanter, S. Catheline, M. Fink, L. Sandrin, C. Cornillon, B. Querleux, *IEEE Trans. Ultrasonics, Ferroelectrics and Frequency Control* **2004**, *51*, 980.
- [26] Y. Kim, J. Zhu, B. Yeom, M. D. Prima, X. Su, J.-G. Kim, S. J. Yoo, C. Uher, N. A. Kotov, *Nature* **2013**, *500*, 59.
- [27] R. Agha, R. Ogawa, G. Pietramaggiore, D. P. Orgill, *J. Surgic. Res.* **2011**, *171*, 700.
- [28] H. Haiying, *Sens. J., IEEE* **2013**, *13*, 3865.
- [29] a) S. H. Song, J. H. Park, G. Chitnis, R. A. Siegel, B. Ziaie, *Sens. Actuators B: Chem.* **2014**, *193*, 925; b) R. Koseva, I. Mönch, J. Schumann, K. F. Arndt, O. G. Schmidt, *Thin Solid Films* **2010**, *518*, 4847.
- [30] a) X. Li, D. R. Ballerini, W. Shen, *Biomeicrofluidics* **2012**, *6*; b) D. D. Liana, B. Raguse, J. J. Gooding, E. Chow, *Sensors* **2012**, *12*, 11505.